Université Paris Saclay

M1 Magistère de Physique Fondamentale

Time Resolution Studies for LHCb ECAL Upgrade II

Rédigé par:
Émile Caire
Magistère de Physique

Tuteur de stage:
Aleksandar Bordelius
Loris Martinazzoli
CERN

Début du stage: 10 Juin 2024
Fin du stage: 30 Août 2024

Abstract

Abstract in English

I was selected (among 10,000 + applications) to participate in the CERN Summmer Student program in Geneva. During my twelve week internship at CERN, I worked with the LHCb ECAL Upgrade II team. My project was focused on time resolution studies on several modules of the new electromagnetic calorimeter (ECAL) for the LHCb experiment. The project started with two weeks on test beam at SPS facilities from CERN, where different prototypes where studied. Once the results from test beam were available, I was in charge of time resolution analysis. I studied different prototypes and obtained interesting results that will be presented during this report.

Résumé en Français

J'ai ete selectionné (parmi 10,000 + de candidatures) pour participer dans l'école d'été du CERN à Genève. Pendant mon stage de douze semaines j'ai travaillé avec le groupe LHCb ECAL Upgrade II. Mon projet était centré sur des études de résolution temporelle pour plusieurs modules du nouveau calorimètre électromagnétique (ECAL) pour l'expérience LHCb. Le projet a commencé avec de semaines de faisceau test du SPS du CERN où plusieurs protypes ont été étudiés. Une fois ayant les résultats du faisceau test j'ai été responsable de l'analyse en résolution temporelle. J'ai étudié différents prototypes et j'ai obtenu des résultats intéressants que je présenterai dans ce rapport.

Contents

Chapter 1

Introduction

The LHCb (Large Hadron Collider beauty) experiment at CERN focuses on understanding the fundamental differences between matter and antimatter. By studying the decay of beauty quarks (also known as bottom quarks), LHCb investigates why the universe contains more matter than antimatter. This experiment plays an important role in exploring CP violation, a phenomenon that could explain the matter-antimatter asymmetry in the universe.

The Electromagnetic Calorimeter (ECAL) in the LHCb experiment is an important subdetector designed to measure the energy of electrons and photons produced during particle collisions. Located between the RICH2 detector and the hadronic calorimeter HCAL, ECAL is composed of alternating layers of scintillating material and lead. When high-energy particles pass through, they generate showers of secondary particles, which produce light in the scintillator. Photodetectors such as Photomultipliers Tubes or PMTs, then convert this light into electronic signals, allowing precise measurement of the particles' energy. ECAL's data is vital for identifying and studying physics channels with electrons and photons, and to distinguish said particles from hadrons.

1.1 ECAL Upgrade II

Important upgrades for the ECAL are expected during long shutdown 3 and 4 of the LHC. The new High-Luminosity phase of the LHCb is expected to have a luminosity of 1.5×10^{34} cm^{-2} s^{-1} for LS4. For the ECAL, a replacement of the innermost modules, which will be affected by radiation damage incurred by the end of Run 3, is proposed, using a new design based on SpaCal technology (see Figure 2.1) for LS3. Additional timing capabilies of $O(10)$ ps will be added to the SPACAL for LS4 modules to keep up with the increase of the number of events due to a higher pile up rate.

Chapter 2

Fundamentals

Electromagnetic calorimeters are very common in high energy experiments, specially at the LHC. These detectors measure the energy of electromagnetic particles, namely electrons and photons. They are part of a group of different detectors essential to the analysis of particle collisions at CERN.

2.1 Calorimetry in High Energy Physics

These detectors work by absorbing incoming high-energy particles, which interact with the dense material, typically lead or similar heavy metals, causing a cascade of secondary particles, a process known as an electromagnetic shower. As these secondary particles travel through layers of scintillating material, they generate light. When high-energy particles enter a scintillating material, they interact with atoms, causing ionization and excitation. As these excited atoms return to their ground state, they emit photons, producing visible light. This light is a result of the energy released during the de-excitation process. This light is then captured by photodetectors, such as photomultiplier tubes, and converted into an electronic signal. The amount of light produced is directly proportional to the energy of the original particle, allowing for precise energy measurement.

There are many types of sampling calorimeters, one of them being the Sashlik technologies that is a set of absorber plates and scintillating plates that are perpendicular to the direction of the beam (see Figure 2.2). These modules, are the ones that are currently used in the LHCb ECAL with over 3000 modules. The new modules that are being studied are the Spaghetti Calorimeter or SpaCal modules. These modules use a unique structure of scintillating fibers inserted in a lead or tungsten matrix, these fibers provide high granularity and precise time measurement. The SpaCal design improves the ECAL's ability to precisely measure the energy of electrons and photons while being in high-radiation environments.

2.2 SPACAL technology

New SpaCal modules will be added to the inner-most region of the calorimeter. This technology will allow to absorb higher doses of radiation (around 1MGy). These modules are expected to keep the same energy resolution as the Shashlik modules of :

$\frac{\sigma(E)}{E} = \frac{10\%}{\sqrt{E}} \bigoplus 1\%$ Moreover, the SpaCal modules are expected to have timing capabilities for LS4 that can distinguish between two events with a precision of around 10 picoseconds. This added timing resolution will enhance the system's ability to differentiate various events from background noise. Time information can help combat the pile-up and improve the energy resolution in the clustering algortihm.

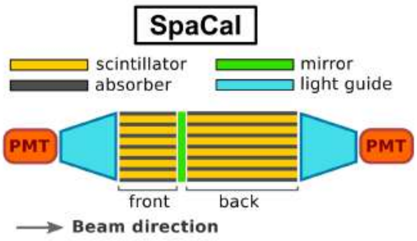

Figure 2.1: SpaCal module scheme

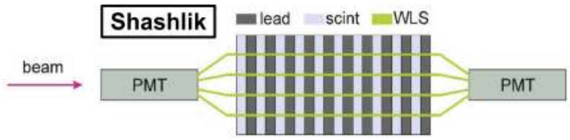

Figure 2.2: Shashlik module scheme

2.3 Time Resolution

The High Luminosity phase of the LHC will increase the number of collisions per bunch crossing, resulting in more events to analyse. In order to keep up with this rate, fast detectors and fast electronics are needed. To study specific events, during the analysis, several parameters are used to distinguish the signal of the studied event and the backgound (see Figure 2.3).

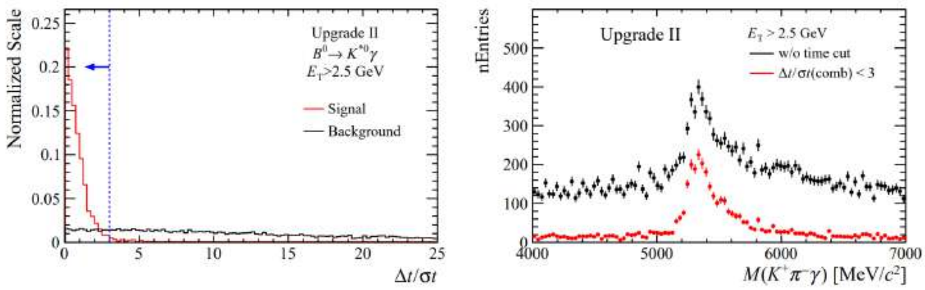

Figure 2.3: (Left) Comparison of the time properties for signal and background candidates in the $B^0 \to K^{*0}\gamma$ simulation. Here Δt is the difference between the measured and expected arrival times of the photon and σt is the time resolution, which depends on the photon energy and the relevant ECAL region; the vertical dashed line indicates the region selected by the time window cut. (Right) Mass spectrum for $B^0 \to K^{*0}\gamma$ simulated events selected with and without the time window applied around the expected arrival time of the photon. **Source : LHCb TDR 023 [1]**

Performance on timing capabilities for the SpaCal modules is done in test beams. Test beams for PicoCal group generally take place in the North Area at SPS at CERN, or at DESY in Germany. A SpaCal module is placed in front of a beam of electrons and the time, position and the energy of each electron is measured. Time resolution can be written as follows :

$$\sigma_t(E) = \frac{A}{\sqrt{E}} \bigoplus B \tag{2.1}$$

The stochastic term **A** arises from the statistical nature of the particle interactions within the calorimeter, such as the fluctuations in the number of photons detected, their spread in production and travel. This term decreases with higher energy, as more particles contribute to the measurement, improving the precision. The constant term **B**, on the other hand, represents the inherent limitations of the calorimeter, such as the precision of the electronics, alignment, and calibration stability. Unlike the stochastic term, the constant term does not improve with energy and sets a baseline for the best possible time resolution achievable by the calorimeter. See [2].

Chapter 3

Experimental elements - Test Beam

3.1 Experimental setup

The main point of this test beam is to study different prototypes with a controllable beam of which all characteristics such as energy are well known. In figure 3.1 we can see the experimental setup. The beam pipe is aligned with a series of detectors that will allow us to study the performance of the prototype. Among the detectors there is :

- **Beam pipe :** Where the elctrons (or pions) come from SPS, energies used range from 20 GeV to 100 Gev.
- **Scintillator pads :** These will be the trigger for the measurement.
- **2 Microchannel Plate Detectors (MCPs) :** The origin in time for our measurement or the reference.
- **3 Delay Wire Chambers (DWCs) :** To measure the position of each electron passing through the detector.
- **Metal box :** The prototype will be fixed inside a metal box. Inside the box are all the cables that link the PMTs to the electronics.
- **DAQ & Electronics :** One ADC module and one digitizer converting the signals from the PMTs into exploitable data.

Figure 3.1: Experimental setup at SPS

3.2 Constant Fraction Discriminator technique

The Constant Fraction Discriminator (CFD) technique is a method used in signal processing to accurately determine the timing of a pulse, regardless of its amplitude. In detectors like those used in high-energy physics, signals from particles can vary in height due to fluctuations in energy (due to the energy variety of the detected particles), but the time at which the particle interacts with the detector must be measured precisely. The CFD technique addresses this challenge by triggering not at a fixed threshold but at a constant fraction of the pulse's peak amplitude. Here's how it works: The timestamp is not measured at a fixed amplitude threshold but rather a fraction of the amplitude (e.g 30%) The threshold is then independent of the pulse's amplitude, allowing for precise time determination. See [3].

3.3 The analysis

After data collection, the waveforms are analysed extracting quantities like integral, amplitude, timestamp with CFD . . . This is later used to analyse and create all the plots on time and energy resolution. I will briefly explain the idea of time analysis done during my summer project.

Each event will produce a waveform as can be seen on Figure 3.2. In this waveform we can read the amplitude of the signal in the *y axis* and the time in nanoseconds in the *x axis*. We extract three crucial information which are **the baseline** in blue, **the amplitude** in red and **the timestamp** in green. Notice that the timestamp is taken at the value of the CFD which is 30% of the amplitude here.

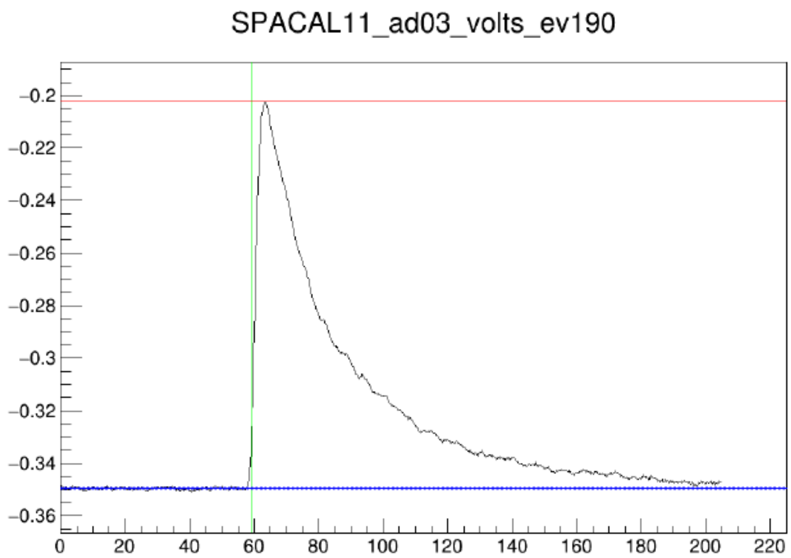

Figure 3.2: Example of a raw waveform of one event

For time resolution analysis we foccus mainly on the timestamp but the other values are good indicators in case there is a problem with the measurements. Once we have the timestamp, we subtract the reference time, which is the simple mean of the time recorded by the MCPs. With subtracting the reference we set a time frame of reference for the events as timestamps alone are arbitrary and can fluctuate largely event by event. We plot a histogram for all the values of every event and we divide the results into channels (which in this case one channel is one cell). In figure 3.3 we can see the final histogram for WGAGG prototype at 20 GeV for cell 11.

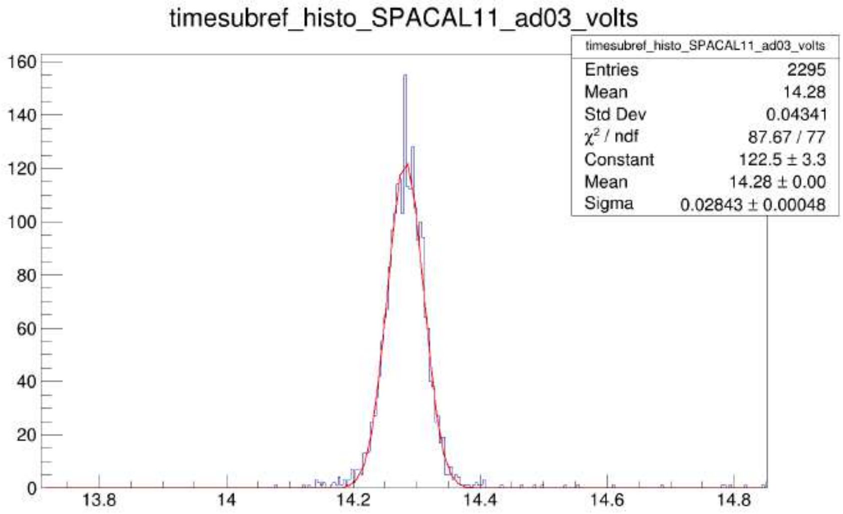

Figure 3.3: Example of time histogramm for WGAGG module

In order to obtain time resolution a gaussian curve is fitted and the standard deviation of the fit is the time resolution. As to obtain the stochastic and constant terms, a plot with time resolution for different energies is needed and that will be presented in the next chapter.

Moreover, in the analysis the time resolution of the reference is also computed and later subtracted from the fit of the histogram. This allows us to analyse the intrinsic performance of the prototype without limitations in time resolution from the reference itself, as the instrument used as the reference, the MCPs are not an ideal detector. The plots of time resolution that will be presented in this presentation, all have the reference subtracted.

2D maps and DWC

Delay wire chambers (DWC) are a type of particle detector used to determine the position of charged particles in an experiment. They consist of a series of parallel wires placed in a gas-filled chamber. When a charged particle passes through the chamber, it ionizes the gas, creating free electrons. These electrons drift toward the nearest wire, inducing a signal. The time it takes for the signal to reach the end of the wire is proportional to the particle's position along the wire. By measuring these delays on multiple wires, the chamber can precisely determine the particle's trajectory and timing within the detector.

For the analysis, it is interesting to visualize the prototype with a 2D map. The DWC will record the position where the particle will hit the prototype. With the x and y information a 2D plot can be made with *ROOT* that can be used to check homogeneity in amplitude or time resolution in the prototype. This analysis will be explained further on in section 4.3.

Chapter 4

Test Beam Results

4.1 WGAGG Prototype

This prototye has a tungsten absorber and scintillating crystal fibres. It has a double-sided readout configuration as seen in Figure 4.2. This means that the module is separated in two parts with a mirror placed at the shower maximum. The shower maximum is the point in the calorimeter where the number of secondary particles (and thus the energy deposition) is at its highest. Beyond this point, the number of particles begins to decrease as the particles are absorbed or escape the detection volume. Each cell has two readout channels so there are 32 channels in total.

In order to do time resolution analysis for this prototype, one must consider a way of combining information from two channels in order to reconstruct time resolution in one cell. One solution proposed is to take the weighted average of time resolution with the weights being the amplitude of the signal. That way, particles with higher amplitude will have a bigger weight and time resolution should improve.

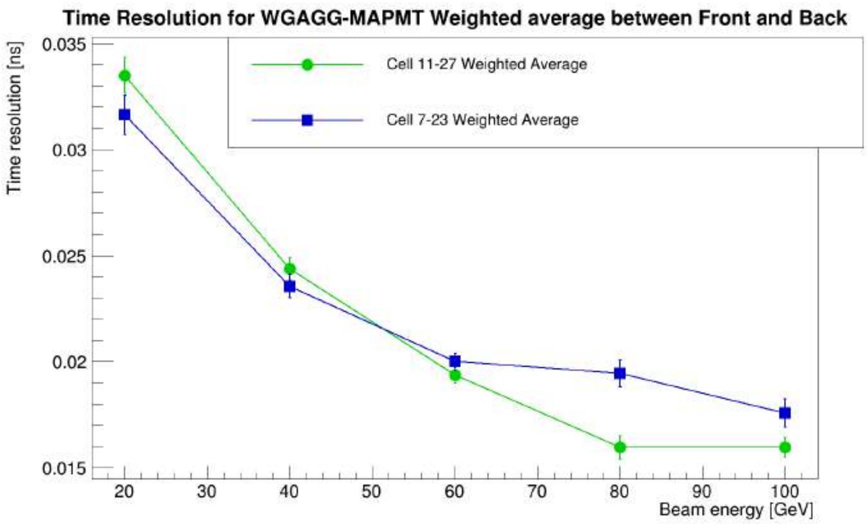

Figure 4.1: Comparison between two cells for WGAGG

In figure 4.1, we present the results for time resolution obtained for two different cells taking the weighted average between front and back. These two cells are identical so the time resolution should be the same, which is the case up to a certain error.

4.2 Pb Poly Prototype

This prototype was built and tested during my summer student internship. With a single-sided readout (contrary to the WGAGG prototype, Pb Poly has only the back part). Pb Poly has 16 cells of 30 × 30 mm^2 surface and green scintillating fibres from Kuraray SCSF-3HF inserted into a lead absorber. A hollow plastic light guide is placed at the end of the module to optically link the output to the PMTs. A highly reflective material (ESR) is placed inside the plastic frame. Please note that other materials than plastic are being studies as candidates for the experiment. It is important to note that the fibres are bundled at the end, before the light guide, this has shown good results in energy and time resolution that can be explained from a better light yield. See pictures from this prototype in Annex A.1.

4.2.1 Comparing two PMTs

As we saw previously, time resolution depends on many factors. Its constant term is highly linked to the performance of the detectors and its electronics. During the analysis of the Pb Poly prototype two PMTs were tested (see Figure 4.2 and 4.3). For simplicity purposes we will refer to them as "square PMT" and "small round PMT". Different runs were made shooting at 4 different sections of cell 11 at 5 different energies. This allowed us to exctract every standard deviation from time histograms (see section 3.3) for each energy and get a final plot on the behavior of time resolution with respect to energy.

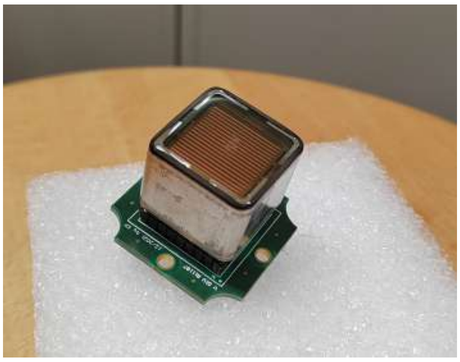

Figure 4.2: Square PMT (Hamamatsu R11187)

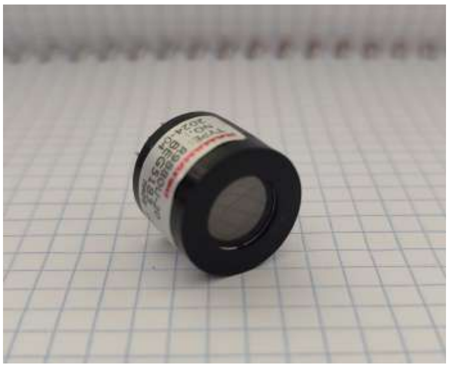

Figure 4.3: Small round PMT (Hamamatsu R9980U)

Using the algorithm explained in section 3.3 we plot the time resolution as a function of energy and we fit using the equation 2.1. We obtain the time resolution curves for both PMTs as seen in Figure 4.4.

Here we can see that the Square PMT has an overall better time resolution. In the stochastic term there is an 80% difference between the two PMTs. This could be explained by the amount of light each of the PMTs will get at the end. Indeed, the amount of light a PMT receives can be quantified as Light Yield. Some light yield measurements were done by the group and the results will be presented in the next section.

Light Yield measurements

Light yield measurements on Photomultiplier Tubes (PMTs) assess the amount of light produced by a scintillating material when it interacts with a particle, which the PMT then converts into an electrical signal. To measure light yield, a known source of radiation is used to excite the scintillator, generating light. This light is then captured by the PMT,

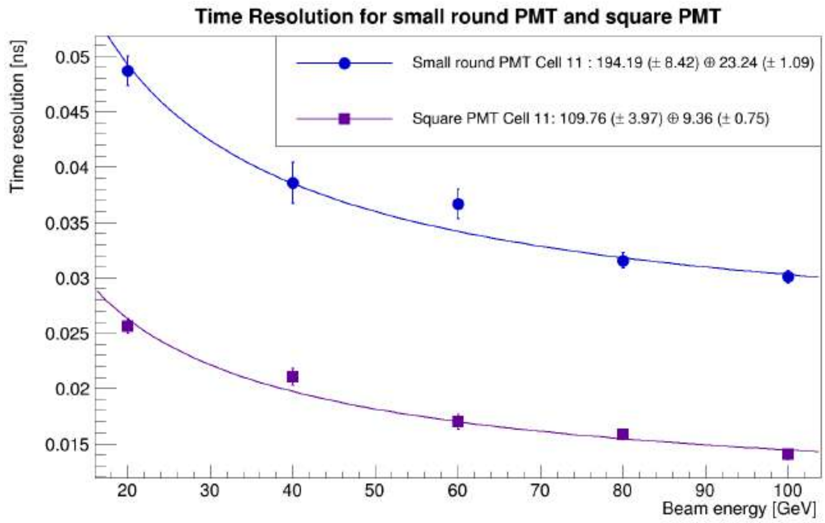

Figure 4.4: Time resolution comparing two PMTs

which converts it into an electrical pulse. The strength of this pulse is proportional to the amount of light produced. By analyzing the amplitude of these pulses, the light yield can be quantified, often in terms of the number of photoelectrons produced per GeV. This measurement takes into account the quantum efficiency of the detector. It is important to note that the two PMTs studied here do not differ by a lot in terms of quantum efficiency. The loss of light detected can be explained specially by the light guides used during the experiment. Light guides play an important role in time resolution and the amount of light that is detected. Several studies are being done on light guides. Light yield of the detector seems to have a strong dependence on the geometry of the light guide (e.g length and shape). For these two PMTs, light yield measurements were done by the group during test beam with the following results :

Light Yield Measurements	Square PMT	Small Round PMT
Number of photoelectrons per GeV	1004	294

Table 4.1: Light Yield measurements results

In Table 4.1 we can see that $LY_{Small-Round} = 0.3 \cdot LY_{Square}$. These values can be linked to time resolution via the formulas

$$\sigma_{Square} = \frac{1}{\sqrt{LY_{Square}}}$$

and

$$\sigma_{Small-Round} = \frac{\sigma_{Square}}{\sqrt{0.3}} = 1.83 \times \sigma_{Square}$$

Then, we can trace an adjusted function using the formula from equation 2.1 and we obtain two curves fitting two constant terms for the PMTs (see figures 4.5 and 4.6). It is important to note that for the curve with the adjusted light yield and the constant term for the square PMT we do not have a perfect match with any of the curves. The effect on the constant term is still something to be understood. This can vary between different Light Guides or from different configurations.

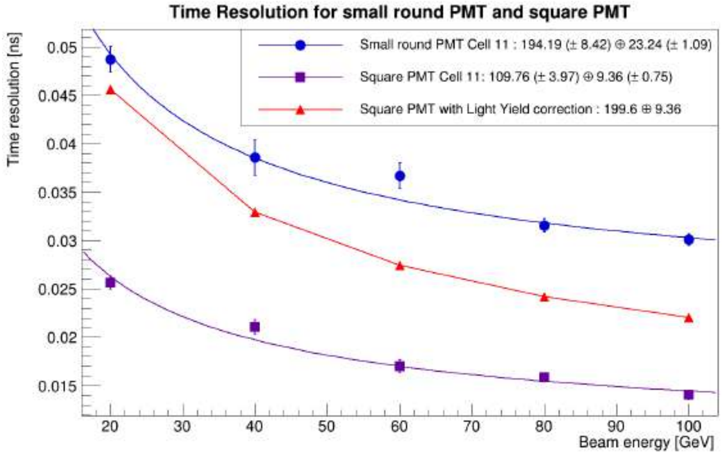

Figure 4.5: Time resolution with adjusted Light Yield 1

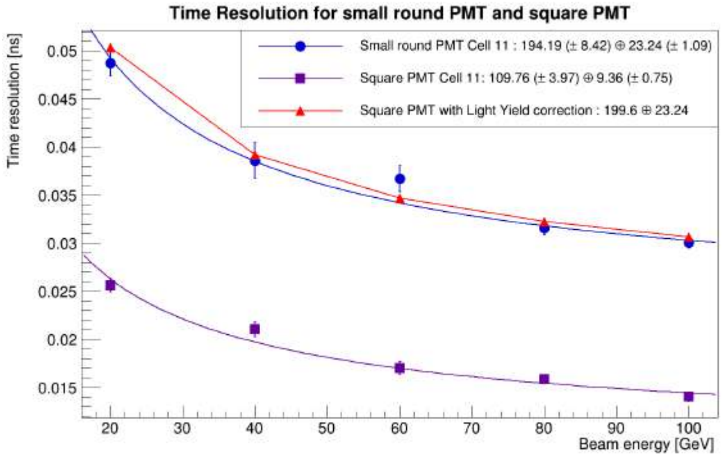

Figure 4.6: Time resolution with adjusted Light Yield 2

4.2.2 Multi Cladding vs Single Cladding fibres

For the PbPoly prototype green scintillating fibres from Kuraray SCSF-3HF were used. These fibres come in two different configurations with **single cladding** or **multi cladding**. They have a scintillating core and then a cladding on top to keep the light inside the fibre. The cladding is made of material with a lower refractive index than the core, which ensures that light stays within the core by reflecting off the cladding, thereby guiding the light through the fiber. Single cladding is simpler and generally less expensive to manufacture. Multi-cladding fibers have a more complex structure, involving multiple cladding layers around the core. Each cladding layer has a different refractive index, which can be designed to manipulate light in more sophisticated ways. This can include optimizing light confinement, reducing losses and have a better expected light yield.

This prototype of Pb Poly has 15 cells with multi cladding fibres and 1 cell with single cladding. The object of my research was to compare the different characteristics from these two types of fibres from the point of view of timing.

When doing time resolution studies it is interesting to work directly with the waveforms from two different configurations. From the waveforms one can compare the rise time which is the time it takes for the signal to go from 10% to 90%. To simplify this study and not to compare every waveform produced by each event, we make an average waveform from

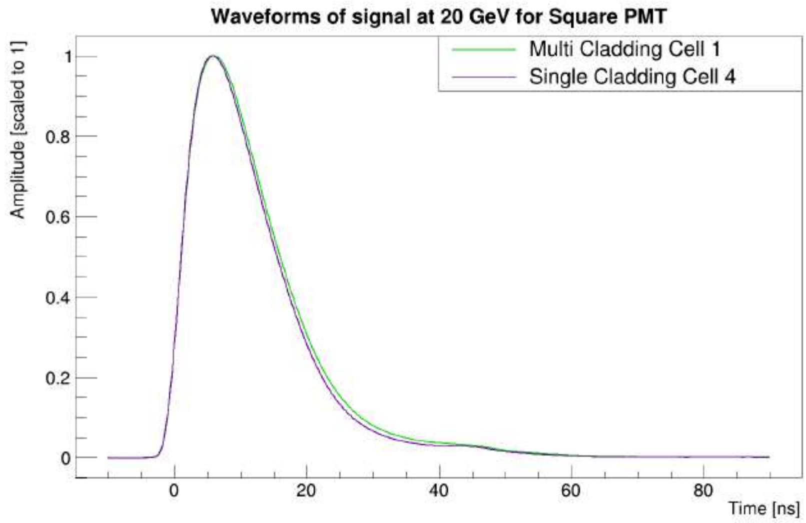

Figure 4.7: Waveform between single and multicladding fibres

all the data of the studied cell and compare. In figure 4.7, we can compare the waveforms from single cladding and multi cladding fibres for 20 Gev. We can already detect that single cladding fibres seem to have a faster pulse. In figure 4.8, we plot the rise time of each average waveform for different energies.

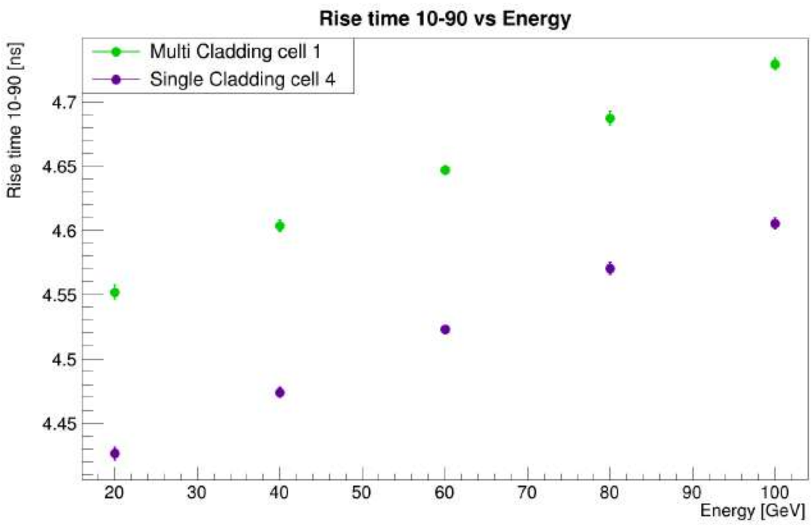

Figure 4.8: Rise time between single and multicladding fibres

Finally, we plot time resolution for single cladding and multi cladding cells at different energies as seen in figure 4.9. Here, we see that both cells have similar time resolution with a slight improvement for single cladding cells. This result is interesting as single cladding cells are 30 % cheaper than multi cladding, and if they have the same performance in time resolution it could be a very good candidate for the modules that will be used in the experiment. These results remain very preliminary but further study of single cladding cells remains important.

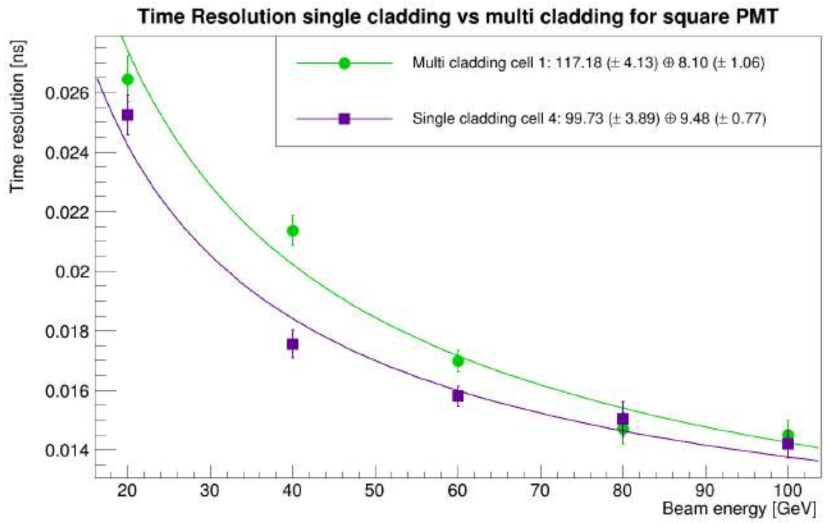

Figure 4.9: Time resolution for single and multi cladding fibres

4.3 Time Homogeneity map

For my final project, I was given the task to investigate more on time homogeneity in the prototype. I had to modify the existing analysis algorithm in order to include a 2D map of the time measured . As seen in Section 3.3, the delay wire chamber allowed us to record the position at which the particle hits the cell. This information is then used to make spatial cuts on the analysis to select only the cells that we are studying. Measurements were made focusing the position of the beam at the border of the cell to study if there was any effect on the border.

Aligning in time + merging data + taking square weighted average

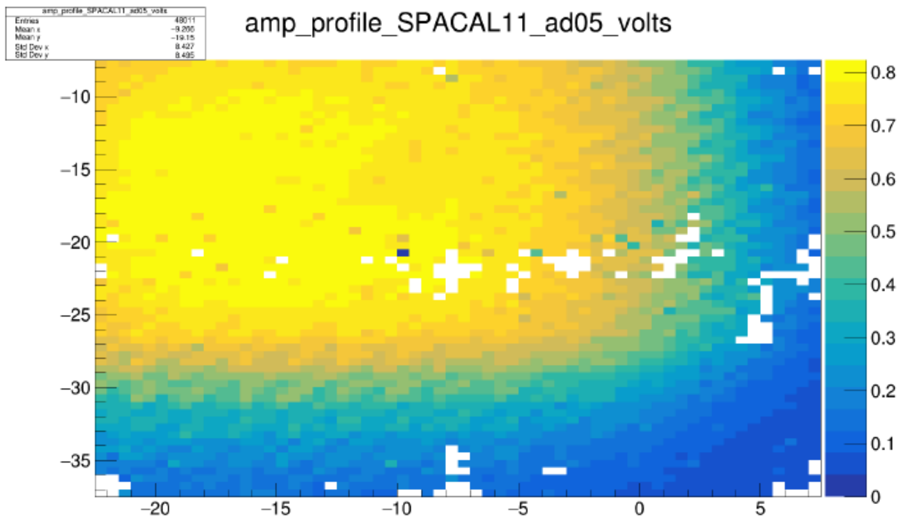

Figure 4.10: 2D Profile of the amplitude

The amplitude of the signal can be visualized in a 2D map in Figure 4.10. Here is a reconstruction of 4 runs hitting the lower border of cell 11. With this type of analysis one can visualise the position of the cell and the effect on the borders. The most yellow marks the position of the cell and we can see a decrease on amplitude as we move towards the neighboring cells. The objective of the project is to study if this effect is also present for timing studies at the border of cells. In the ideal case, the prototype would have an homogeneous timing of events all over its surface.

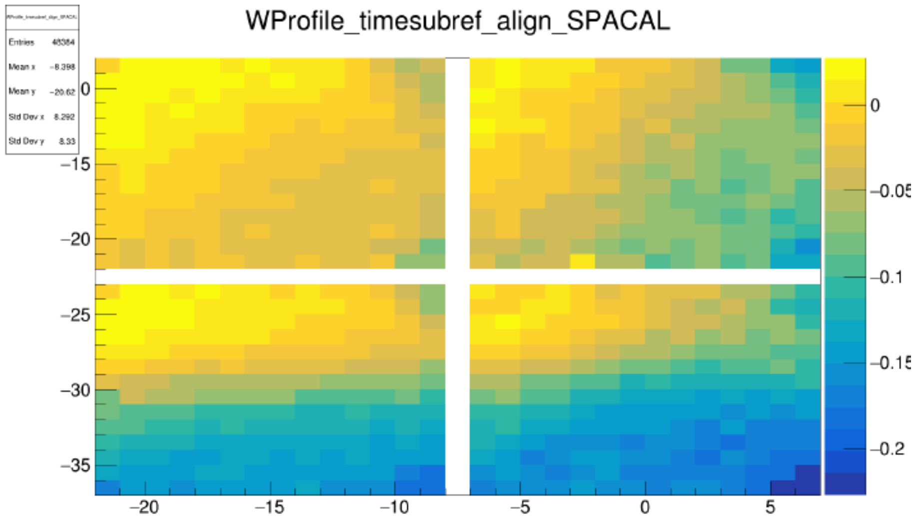

Figure 4.11: 2D Profile of recorded time with spacial cuts

For this timing analysis, ideally, the information from all the channels has to be taken into account. To do this, for every event, we take the weighted average of the time measured by every channel with the weights being the amplitude of the signal. Then we divide this value by the sum of the amplitudes of every channel. For example, to compute the time of cell 11 taking into account the signal from cell 10 we would use the formula :

$$t = \frac{a_{11}}{sum} \cdot t_{11} + \frac{a_{10}}{sum} \cdot t_{10}$$

Where *sum* is the sum of the amplitude of both channels $a_{11} + a_{10}$. To consider the effect of the other channels we add their contribution and add the amplitude into the sum.

Some modifications were necessary for this to work. In the end a map of relevant channels was needed, not all channels were taken into account. This is due to some irregularities and outliers present in the measurement at very low amplitude. A squared average was used to minimize the impact of these outliers but this was not sufficient, so only some selected channels were taken into account. Furthermore, the time histograms were shifted to have zero average before computing. We noticed that cells were not aligned in time, there was no calibration in time done during test beam for the PMTs so to subtract this effect, all time histograms were centered in zero.

Finally we obtain the results from figure 4.11. Please note that the cross in the middle is due to spacial cuts that were done during the analysis. In this 2D graph the timescale is in nanoseconds. We can see that the prototype has an homogeneous time with a variation on 200 ps. We can take two things from this result. First, comparing this figure with the amplitude profile from Figure 4.10, we can see a similar shape recognizing the borders of the cell. With the decrease in amplitude at the border of the cell comes a shift in time and we see the structure of the cell. Finally, on the plot one can see a round silhouette forming around each quarter. This could be explained by the presence of the MCPs. In this case seeing the effect of the MCPs could mean that the results are biased by the time resolution of the MCPs and that we cannot see the intrinsic behaviour of the prototype. Further analysis is needed to understand this effect and to improve time homogeneity studies in the detector.

Chapter 5

Conlusion

In conclusion, this report outlines the research undertaken during my summer student internship in the development and testing of the electromagnetic calorimeter (ECAL) for the LHCb ECAL Upgrade II. The research, primarily focused on time resolution studies, explored the performance of various prototypes, including the WGAGG and Pb Poly modules. Test beam experiments, coupled with rigorous data analysis, provided insights into key aspects such as the impact of different photomultiplier tubes (PMTs), and the comparison between single and multi-cladding fibers.

One of the main findings was the improved time resolution achieved using square PMTs, offering better performance than their smaller counterparts, a result closely tied to light yield measurements. Furthermore, the comparison between single and multi-cladding fibers revealed that the former offered a slightly better time resolution, while being a more cost-effective option. This opens up possibilities for using single cladding fibers in future ECAL designs without compromising performance.

The analysis also included a homogeneity study, highlighting that while amplitude decreases at the edges of the cells, the time resolution remains largely uniform across the prototype. However, further research is needed to fully understand the influence of the reference detectors, such as the MCPs, on the timing homogeneity.

Overall, the results of this report contribute valuable data towards optimizing the ECAL for future runs of the LHCb experiment, with the goal of achieving higher precision in time measurements.

Appendix A

Photos from the prototypes

A.1 Pb Poly Prototype

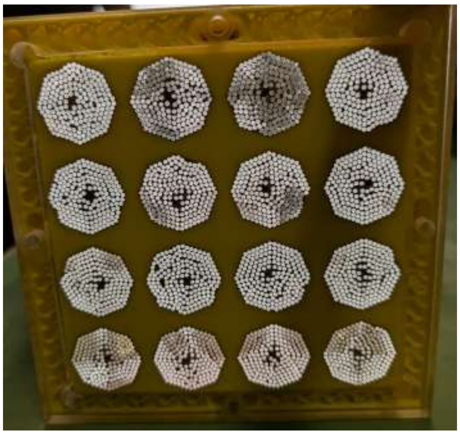

Figure A.1: Pb Poly Bundled fibres

Figure A.2: Full Pb Poly Prototype

Figure A.3: Pb Poly light guide

A.2 WGAGG Prototype

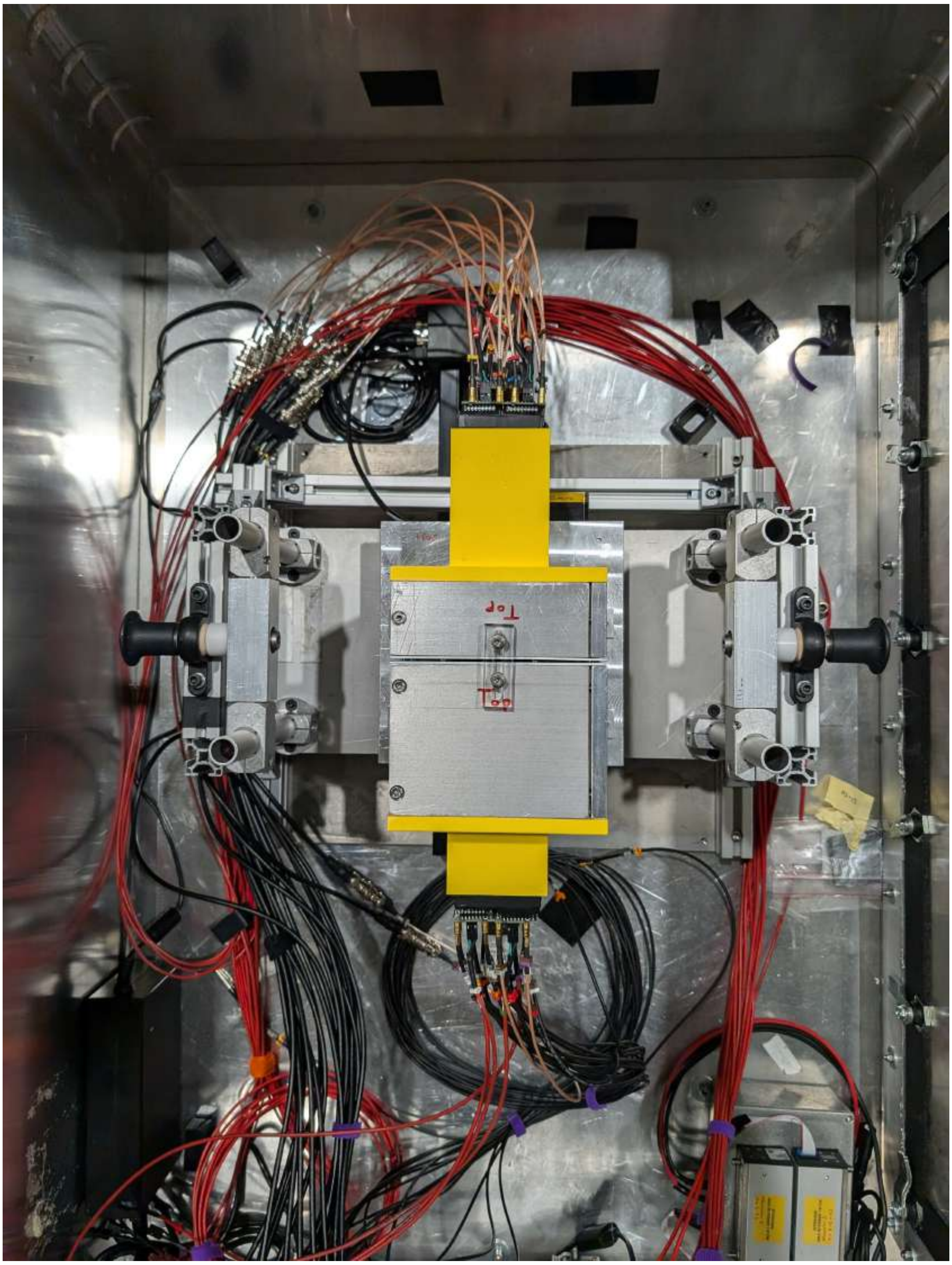

Figure A.4: WGAGG Protype in test beam

Acknowledgements

First of all, I would like to thank my two SUPERvisors Alex and Loris. It is thanks to them that I had this once in a lifetime opportunity of working at CERN. It has always been my dream to work in a major laboratory of physics and they made that dream come true. I have learned so much from them and they were always kind and available for me.

During this summer, I met the most amazing and interesting people, from whom I learned so much. I would like to thank all of my other summer student friends that I made along this journey.

I would like to thank the HR summer student team Anastasija, Tereza, Kristin and Ernest.

Finally, I would like to thank my parents and my girlfriend Nicole, who have always been there for me, have given me love and support and they are the reason that I am where I am today.

Bibliography

[1] LHCb Collaboration. The lhcb ecal upgrade ii. Technical report, CERN, 2023.

[2] Christian W. Fabjan and Fabiola Gianotti. Calorimetry for particle physics. *Reviews of Modern Physics*, 75(4):1243–1286, 2003.

[3] Loris Martinazzoli for the LHCb PicoCal group. Performance of a spaghetti calorimeter prototype with tungsten absorber and garnet crystal fibres. *Nuclear Instruments and Methods in Physics Research*, November 2022. Preprint submitted on November 9, 2022.